

Simulating Wave-Tide Induced Circulation in Bay St. Louis, MS with a Coupled Hydrodynamic-Wave Model

Mark Cobb

Sverdrup Technology, Inc.
MSAAP Building 9101, Door 136
Stennis Space Center, MS 39529, U.S.A.
cobb@nrlssc.navy.mil

Cheryl Ann Blain

Oceanography Division (Code 7322), Naval Research Laboratory
Stennis Space Center, MS 39529, U.S.A.
blain@nrlssc.navy.mil

Abstract—Because tidal inlets are important areas with respect to bio-diversity, sediment transport, fresh water river outflow, and pollutant transport a comprehensive understanding of their circulation patterns is necessary for their management. This study focuses on modeling the 2D, depth-averaged circulation of Bay St. Louis in the northeastern Gulf of Mexico that is driven by waves and tides using a coupled hydrodynamic-wave model. The wave-tide coupled circulation within the inlet is examined during the flood, slack, and ebb phases of the tidal cycle. The wave height field, current velocity and sea surface elevation are analyzed to determine the effects of wave-current interaction. The influence of the various forcings on bay/inlet circulation is further investigated by the introduction of Lagrangian tracers. Lagrangian tracers are a reasonable indicator of how circulation patterns affect the motion of sediment particles or passive biological organisms such as fish larvae.

Wave-current interaction is simulated by iteratively coupling the depth-integrated ADCIRC-2DDI hydrodynamic model to the phase-averaged spectral wave model SWAN. ADCIRC-2DDI is a fully developed, 2-dimensional, finite element, barotropic hydrodynamic model capable of including wind, wave, and tidal forcing as well as river flux into the domain. The wave-hydrodynamic model coupling is captured through the following approach. First, radiation stress gradients, determined from the SWAN wave field, serve as surface stress forcing in ADCIRC. Elevation and currents computed from ADCIRC are subsequently input into the SWAN model. Between these iterations, the ADCIRC model is run for some appropriately small time interval during which the wave field is held constant. Presently there are no shelf-scale hydrodynamic models that incorporate waves, therefore a coupled model approach is one way of simulating wave-current interaction in bays and inlets. This approach is very flexible, making it possible to couple different wave models to ADCIRC depending on the relevant physics of the domain being studied (e.g. monochromatic wave diffraction vs. multi-spectral wave effects).

I. INTRODUCTION

The nearshore circulation of a bay/inlet system transports sediments and pollutants as well as biological organisms. In order to protect as well as develop these coastal areas, a better understanding of the forces and bay/inlet geometry that produce their circulation is required. Waves and tides are two significant forcing mechanisms in these systems and wave-current interaction is essential for

capturing the combined effect of these forces in a bay/inlet system [1]. Although wind is an important forcing mechanism of the circulation as well, the focus of this study is on forcing mechanisms that couple to each other.

The effect of wave-current interaction on wave-tide driven circulation in Bay St. Louis, MS is investigated using a coupled hydrodynamic-wave model. An iterative coupled hydrodynamic-wave model has been developed using the depth-integrated ADCIRC-2DDI finite element hydrodynamic model and the 2D spectral SWAN wave model for simulating wave-current interaction in a tidal inlet. This approach was applied successfully in a previous study that examined wave and tidally forced circulation in an ideal inlet geometry [1]. The wave fields, surface elevations, and currents as well as the motion of passive Lagrangian tracers are examined in order to characterize the influence of the different forcing mechanisms and the effects of wave-current interaction on the circulation.

II. CIRCULATION AND WAVE MODELS

Sea surface elevation and coastal currents are modeled using the fully nonlinear, two-dimensional, barotropic hydrodynamic model ADCIRC-2DDI. The ADCIRC (ADVanced CIRCulation Model for Shelves, Coasts and Estuaries) model, developed by [2] and [3], has a successful history of tidal and storm surge prediction in coastal waters and marginal seas ([4], [5], [6], [7]). The depth-integrated shallow water equations, derived through vertical integration of the three-dimensional mass and momentum balance equations subject to the hydrostatic assumption and the Boussinesq approximation, form the basis of the ADCIRC-2DDI model (Note: 2DDI stands for two dimensional depth-integrated). A spatially variable surface stress forcing is determined from the radiation stress (S_{xx} , S_{yy} , S_{xy} , S_{yx}) gradients of the wave field [8] obtained from the SWAN wave model. The non-conservative primitive equations expressed in spherical coordinates are

$$\frac{\partial \zeta}{\partial t} + \frac{1}{R \cos(\theta)} \frac{\partial UH}{\partial \lambda} + \frac{1}{R} \frac{\partial VH}{\partial \theta} - \frac{VH}{R} \tan(\theta) = 0 \quad (1)$$

$$\frac{\partial U}{\partial t} + \frac{U}{R \cos(\theta)} \frac{\partial U}{\partial \lambda} + \frac{V}{R} \frac{\partial U}{\partial \theta} - \left(\frac{U \tan(\theta)}{R} + f \right) V = - \frac{1}{R \cos(\theta)} \frac{\partial(g\zeta)}{\partial \lambda} + D_\lambda + \frac{\tau_{s\lambda}}{\rho_0 H} - \frac{\tau_{b\lambda}}{\rho_0 H} \quad (2)$$

$$\frac{\partial V}{\partial t} + \frac{U}{R \cos(\theta)} \frac{\partial V}{\partial \lambda} + \frac{V}{R} \frac{\partial V}{\partial \theta} + \left(\frac{U \tan(\theta)}{R} + f \right) U = - \frac{1}{R} \frac{\partial(g\zeta)}{\partial \theta} + D_\theta + \frac{\tau_{s\theta}}{\rho_0 H} - \frac{\tau_{b\theta}}{\rho_0 H} \quad (3)$$

where t represents time, (λ, θ) are the spherical coordinate directions, ζ is the free surface elevation relative to the geoid, (U, V) are the depth-averaged horizontal velocity components, $H = \zeta + h$ is the total water column depth, h is the bathymetric depth relative to the geoid, $f (= 2\Omega \sin(\theta))$, where Ω is the angular frequency of rotation for the earth and θ is the degrees of latitude) is the coriolis parameter, g is the acceleration due to gravity, ρ_0 is the reference density of water, D_λ and D_θ are the horizontal momentum diffusion/dispersion, $\tau_{s\lambda}$ and $\tau_{s\theta}$ are the applied horizontal free surface stresses (obtained from the wave-induced radiation stress), and $\tau_{b\lambda}$ and $\tau_{b\theta}$ are the horizontal bottom stress components. This set of equations is considered to be time-averaged over a wave period. The primitive equations are transformed into Cartesian coordinates using a Carte Parallelo-grammatique (CPP) cylindrical map projection as part of the solution procedure (a more in-depth discussion of this can be found in [3] and references therein). The parameterizations of the various terms can now be addressed in Cartesian coordinates. Bottom stress terms are parameterized using the standard nonlinear quadratic friction law:

$$\tau_{bxy} = C_f \rho_0 (U^2 + V^2)^{1/2} \mathbf{v} \quad (4)$$

where C_f is the nonlinear bottom friction coefficient and \mathbf{v} is the depth-averaged horizontal velocity vector. The lateral mixing due to diffusion/dispersion is:

$$D_{xy} = \frac{E_h}{H} \left(\left(\frac{\cos(\theta_0)}{\cos(\theta)} \right)^2 \frac{\partial^2}{\partial x^2} + \frac{\partial^2}{\partial y^2} \right) H \mathbf{v} \quad (5)$$

where E_h is the horizontal eddy viscosity coefficient for momentum diffusion/dispersion [9]. The CPP transformation (centered at (λ_0, θ_0)) introduces an additional factor of $\cos(\theta_0)/\cos(\theta)$ for all x-derivative terms.

The wave field used to force the ADCIRC-2DDI model is derived from the 2D multi-spectral SWAN wave

model [10]. The SWAN wave model is based on the wave action balance equation and can simulate wave refraction, shoaling, blocking, and reflection due to bathymetry, sea surface elevations, and currents. SWAN also has the capability of using sea surface elevations and currents as input for the calculation of the wave field. It should be noted that SWAN cannot simulate wave diffraction and therefore its results in regions where diffraction is significant (e.g. an obstacle) will not be accurate. For this initial study SWAN is a suitable wave model. In a future study the effects of wave diffraction on bay/inlet circulation will be investigated using a different wave model. An additional reason for using SWAN is its ability to model domains with complex coastlines, something which can be significantly more difficult (or impossible) with other wave models.

III. METHODOLOGY OF WAVE-CURRENT INTERACTION

Wave-current (w-c) interaction is incorporated into the simulation by iteratively coupling ADCIRC and SWAN. Wave heights and directions computed by the SWAN wave model are interpolated onto the computational nodes of the finite element grid and radiation stress gradients are then determined at each node. The radiation stress gradients are the surface stress forcing for ADCIRC. It should be pointed out that the radiation stress is determined on the finite element grid using the peak frequency of the wave frequency spectrum, thus treating the SWAN wave data as monochromatic. The wave frequency spectrum is chosen to be quite narrow in order for this approach to produce reasonable results. This is not a restriction of the method but a simplification made for this particular investigation of wave-current interaction. For the purpose of this study it is an acceptable approximation. In future studies a more sophisticated approach will be used to capture the full spectral features of the SWAN wave field. The sea surface elevations and currents of ADCIRC-2DDI are used by SWAN to compute a new wave field at each iteration, which is then used to recalculate the nodal radiation stress gradients.

The ADCIRC model is initially run without two-way coupling for a time interval sufficient to obtain a steady state circulation. After this initial spin-up period, two-way coupling is activated and ADCIRC is run forward for a brief time interval, driven by a new static wave field. At the beginning of each iteration SWAN computes a new wave field that incorporates the ADCIRC sea surface elevation and current velocities from the last time step of the previous iteration (or spin-up). The ADCIRC simulation proceeds as before, forced by a new radiation stress field. This process is repeated after every iteration interval. Although it is possible to couple ADCIRC and SWAN at every time step, it is computationally too expensive to do so at the present time.

IV. ADCIRC DOMAIN

The Bay St. Louis computational domain (Fig. 1) was created using coastline data from the NOAA/NOS Medium Resolution Coastline database obtained using the Coastline

Extractor web site (<http://rimmer.ngdc.noaa.gov/coast/>). This is the best resolution coastline database for the area being investigated. The bathymetry used was obtained from the Northern Gulf of Mexico Littoral Initiative (POC: John Blaha at the Naval Oceanographic Office, Stennis Space Center, MS) and has a resolution of six seconds. The range of the bathymetry is from 11.84 to -2.99 meters. To reduce the computational costs of the calculations a non-uniform finite element mesh is employed. As seen from Fig. 2 the mesh spacing has several levels of refinement, the greatest resolution being near the shoreline and the lowest resolution being offshore; the mesh spacing ranges from 789.1 meters to 29.1 meters. It should be noted that some of the finer, more filamentary coastline features of the actual Bay St. Louis are not represented in this domain. It is necessary to have a highly refined mesh near the coastline because the circulation there is more intense and complex than in the offshore region. In addition, because the SWAN wave model obtains its input bathymetry from the ADCIRC domain, it is necessary to resolve the land-sea transition in order for SWAN to obtain realistic results. A no-flow boundary condition that allows for lateral slip is employed for the coastline and island boundaries and the offshore boundary elevation is modulated with specified tidal amplitudes and phases.

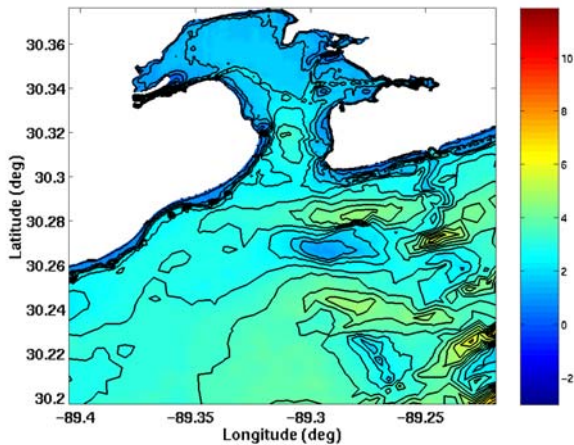


Fig. 1. Bathymetry of the Bay St. Louis domain. The bathymetry contour spacing is 0.5 m with a range from 11.84 to -2.99 meters. The color bar scale is in meters.

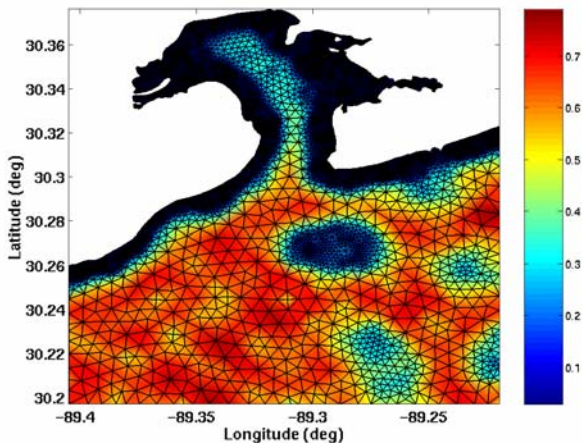


Fig.2. Nodal spacing (in color) of the Bay St. Louis finite element mesh. The color bar scale is in kilometers.

V. SWAN DOMAIN

A regular finite difference (FD) grid with x and y spacing of 39.6 m and 39.9 m respectively is employed for the SWAN computational domain. This results in a rather large computational domain with 225,951 nodes. This resolution is chosen so that the FD grid can resolve the coastline features of the FE grid and in particular the land-sea transition (as discussed in the previous section). The bathymetry SWAN uses is obtained by linearly interpolating the ADCIRC bathymetry to the nodes of the FD grid. If a SWAN node falls outside the ADCIRC domain it is given a depth of -0.01 m, ensuring that SWAN will see a land-sea interface regardless of whether the ADCIRC grid has negative bathymetry at its boundary. The rectangular dimensions of the FD grid encompass the ADCIRC FE grid and normally incident waves propagate inward from the southern offshore ocean boundary. The lateral sides of the outer basin are not closed, allowing waves to propagate out of the domain (but not into the domain).

VI. SIMULATION PARAMETERS

A. SWAN Parameters

The incident wave field has a peak period of 10 seconds and significant wave amplitude of 0.5 m. These parameter values are considered appropriate for coastal wave conditions. It should be pointed out that very little wave data exists in the vicinity of Bay St. Louis and further investigation and/or field studies are required to determine an appropriate incident wave height field for the wave calculation. The peak incident wave direction is specified as 90° since the waves enter perpendicular to the southern boundary of the domain. The default JONSWAP spectrum of the model [10] is used to specify the initial shape of wave spectrum at the boundary. A value of 20 is chosen for the gamma parameter in order to make the spectrum sharply peaked.

B. ADCIRC Parameters

A time step of 4 seconds is chosen for the ADCIRC simulations in order to satisfy the Courant condition [3]. The lateral mixing (E_h) and nonlinear bottom friction coefficient (C_f) are chosen to be $1.0 \text{ m}^2/\text{s}$ and 0.008 respectively. The value of E_h was determined in a previous study to be large enough to prevent the formation of instabilities in the circulation without significantly altering its elevation and velocity values [11]. A relatively large value is chosen for C_f in order to obtain a stable circulation. Without a large friction coefficient, numerical instabilities occur at the land-sea interface on the left lateral boundary of the domain. This is a boundary condition issue that requires further investigation and is beyond the scope of this initial study. For the tidal forcing seven tidal constituents (K_1 , O_1 , P_1 , Q_1 , M_2 , N_2 , and S_2) are used to modulate the offshore boundary elevation. The tidal amplitudes and phases were obtained

from a larger simulation that was performed (by the authors) over the entire Mississippi Bight.

VII. WAVE AND TIDE FORCED-CIRCULATION

To investigate wave-tide coupled circulation a 0.96 day simulation was run in order to observe the main phases (flood, slack, and ebb) of the tidal cycle in the vicinity of the inlet. An initial spin-up phase of 5 days, with a constant wave field forcing, is used to initialize the coupled run. A coupled simulation is then run for 0.96 days (about 23 hours) with an iteration interval of 0.08 days (1.92 hours). In a future study the sensitivity of the circulation to the iteration interval will be investigated. It should be noted though that the results of the previous study [1] indicate that the coupling interval has to be reduced significantly, perhaps from hours to minutes, in order to see pronounced differences in the coupling results. As seen from Fig. 3, the elevation and velocity at a point located in the middle of the inlet have periods of about 1 day for both the tide and wave-tide driven circulation. This indicates that the diurnal components of the tidal forcing are dominant in the vicinity of the inlet. The time intervals of Fig. 3 also match the iteration interval of the coupling (0.08 days).

As mentioned previously, normally incident waves with an initial height of 1.0 m enter the domain from the bottom southern boundary of the domain and propagate into the inlet/bay system. The uncoupled wave height field, shown in Fig. 4, is significantly affected by the shallow bathymetry near the entrance to the inlet (see Fig. 1). The wave height decreases by about 50% or more in this region and thus waves with large amplitudes propagate into the inlet only on its left side (Fig. 4). After entering the inlet the wave heights decrease and are quite small throughout most of the bay. Although, as seen from Fig. 4, the wave height field along the axis of the inlet is still quite significant (approximately 0.5 m) within the bay. Large amplitude waves propagate to the coastline on either side of the inlet as well, breaking in the shallow region near the coastline of the domain.

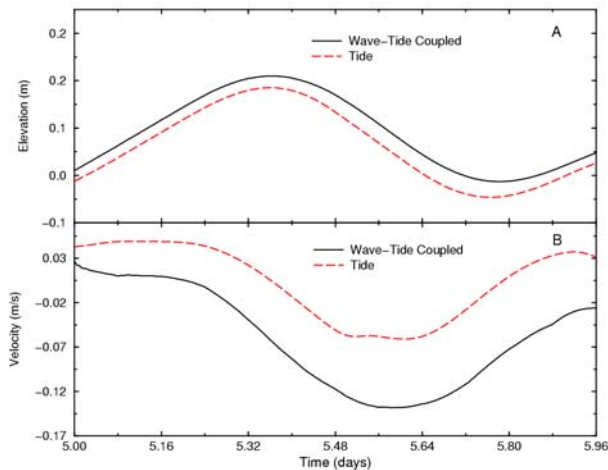


Fig. 3. Time series of tide and wave-tide forced elevation (top) and velocity (bottom) at a point in the middle of the inlet (-89.31°, 30.32°).

An example of the wave-tide coupled circulation during the ebb phase of the tidal cycle (at approximately 5.53 days) is shown in Fig. 5. In Fig. 6 the entrance to the inlet is shown at 5.53 days as well. From Fig. 5 it is apparent that the large scale circulation of the outer ocean region is dominated by the tidally induced currents, but near the coastline the wave-induced currents dominate the circulation. Because the coastline is at an angle to the incident waves strong alongshore current are generated (Fig. 5). Outside the inlet these currents are directed eastward along the coastline, either opposing or enhancing the tidally induced coastal circulation. It is apparent from Fig. 6 that there is a strong wave-induced current flowing into the inlet near the coastline on both sides of the inlet entrance. The tidally induced ebb currents interact with the wave-induced currents to create vortices as seen from Fig. 6.

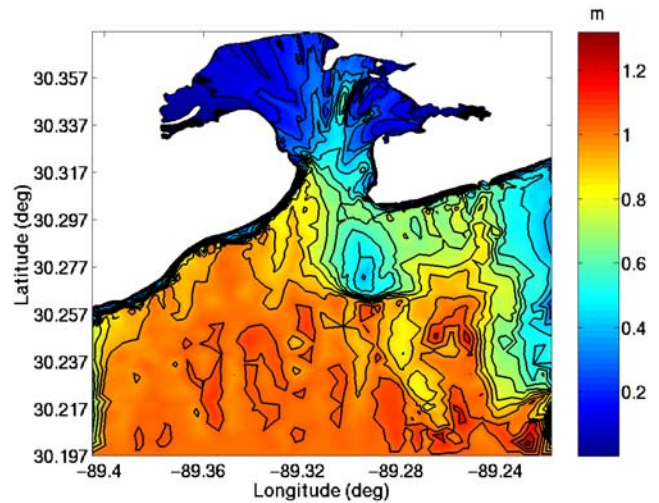


Fig. 4. The uncoupled wave height field used for the spin-up phase of the coupled simulation. Normally incident waves enter from the southern boundary. The contour spacing is 0.08 meters with a range from 0 to 1.32 meters.

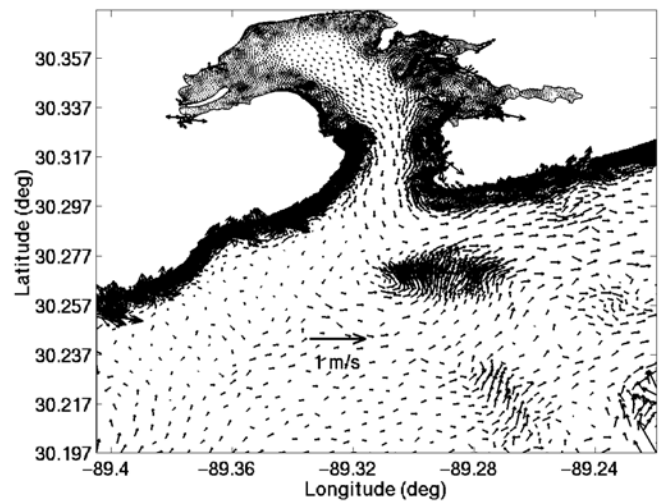


Fig. 5. Current velocity vectors (m/s) for the coupled wave-tide forced circulation during the ebb phase of the tide.

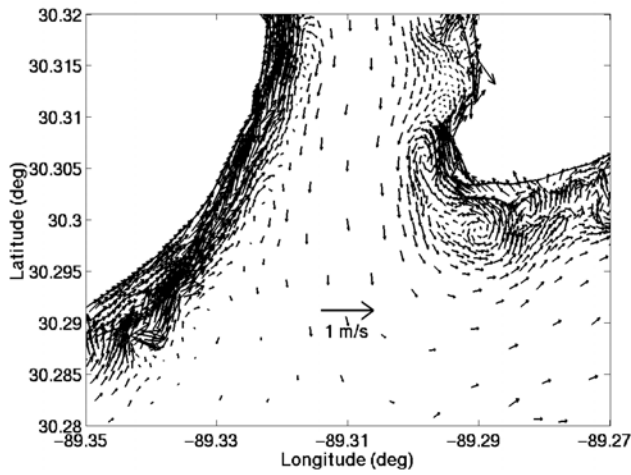


Fig. 6. Current velocity vectors (m/s) for the coupled wave-tide forced circulation during the ebb phase of the tide in the vicinity of the entrance to the inlet.

Because the wave field is updated every 1.92 hours it should reflect the tidally induced changes in the circulation. In Fig. 7 the wave heights for the uncoupled case and the wave-tide coupled case (at flood, slack, and ebb) are plotted along a y-transect (located at longitude = -89.31°) through the middle of the inlet. It should be noted that this is to the left of the shallow bathymetry (previously discussed) near the inlet entrance. The wave heights at ebb for the coupled case, due to the strong outflow through the inlet (Fig. 6), are significantly different from the uncoupled wave heights. The out-flowing current during ebb appears to induce shoaling in the wave field, increasing the wave height. It is interesting that the flood phase wave heights are only slightly lower than the uncoupled and slack phase wave heights. In Fig. 8 the current velocities in the y-direction for the tide and wave-tide coupled cases are plotted at the flood, slack, and ebb phases of the tidal cycle; note that the y-axis is along a line of constant longitude. Examining the current field of the coupled case during the slack phase of the tidal cycle (Fig. 8B) it is apparent that the wave-induced currents create an out-flowing current within the inlet with a peak around 30.30° . The out-flowing inlet current is stronger than the tidally induced flood current, creating an out-flowing current in the middle of the inlet even during the flood phase (Fig. 8A). This current is similar to, but weaker than, the slack phase current in the inlet, resulting in the slightly lower wave heights seen at flood in Fig. 7.

In addition to altering the tidally induced circulation the wave forcing also changes the sea surface elevation. Shown in Fig. 9 are the tide and wave-tide sea surface elevations during flood, slack, and ebb along the same transect used for Fig. 8. At each phase of the tidal cycle there appears to be a difference in tide and wave-tide sea surface height of about 0.02 m at 30.28° . In addition there is wave-induced set-down/up centered around 30.30° (within the inlet) at each phase of the tidal cycle. This is consistent with the decrease in wave height seen in Figs. 4 and 7 at 30.30° . Overall it is apparent from Fig. 9 that the local wave-induced changes in the sea surface are imposed on the large scale

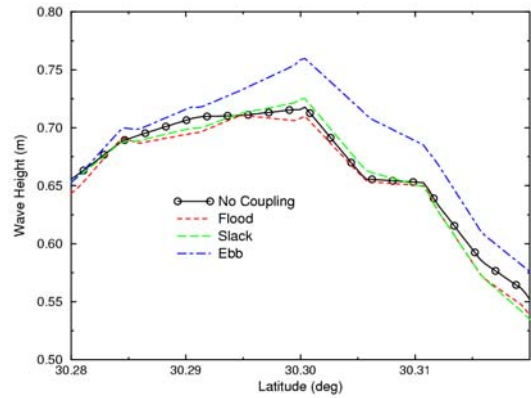


Fig. 7. Wave heights (meters) for the uncoupled (solid with black circles) wave calculation and the flood (dotted), slack (dashed), ebb (dot-dashed) wave-tide calculation along a y-transect at longitude = -89.31° .

tidally induced changes in the sea surface height.

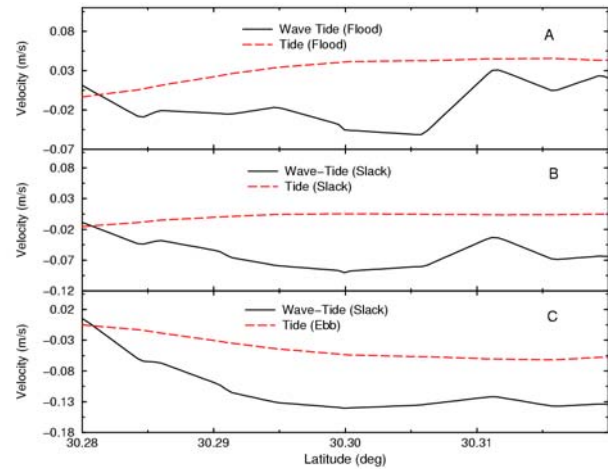


Fig. 8. Tide and wave-tide forced velocity (m/s) in the y direction at the flood, slack, and ebb phases of the tide along a y-transect at longitude = -89.31° .

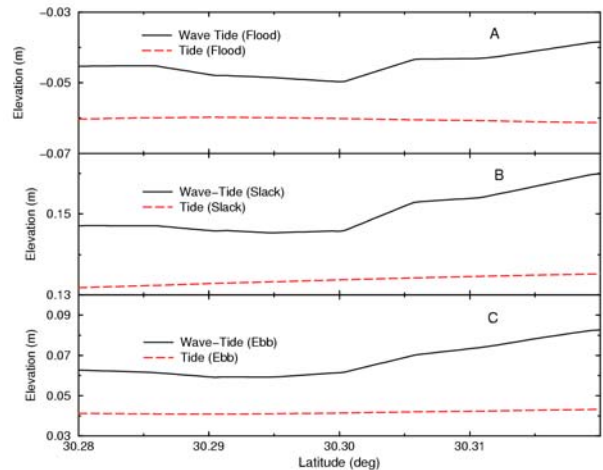


Fig. 9. Tide and wave-tide forced elevation (meters) at the flood, slack, and ebb phases of the tide along a y-transect at longitude = -89.31° .

The transport of passive tracers such as sediments and pollutants is an important aspect of inlet circulation. Passive Lagrangian tracers are used to characterize and compare the transport behavior of the tide and wave-tide forced circulation. In Figs. 10 and 11 the paths of passive Lagrangian tracers, moving under the influence of tide and wave-tide forced circulation respectively, are shown for a time period of 0.96 days (that starts at 5.0 days). The tracers are initially positioned across the middle of the inlet along a horizontal transect and their paths are determined using time slices of the velocity field. The temporal resolution of the velocity fields are 144 seconds and 72 seconds for the tide and wave-tide cases respectively.

In the tidal circulation the tracers essentially return to their initial starting point and begin another cycle. The motion of the tracers is quite different in the wave-tide driven circulation as seen from Fig. 11. The tracers move along the wave-induced currents to locations far from their initial starting points. As discussed previously there is a wave-induced out-flowing inlet current that is significantly stronger than tidally induced flood currents. There are also very intense wave-induced inflowing currents along the sides of the inlet. It is apparent from Fig. 11 that the tracers near the sides of the inlet move (at least initially) into the bay with these currents. Some of these tracers are eventually flushed out of the bay along the out-flowing current. Tracers near the middle of the inlet follow the out-flowing current into the outer ocean region. In addition, some of the tracers on the right side of the inlet are caught up in a strong eddy and do not exit the bay.

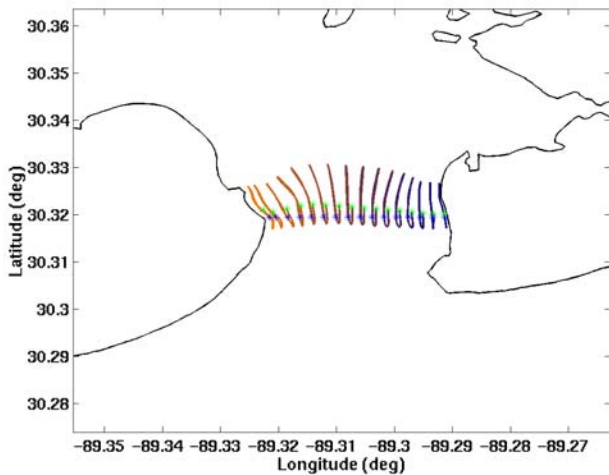


Fig. 10. The paths of passive Lagrangian tracers moving under the influence of tidally-driven currents over a time period of 0.96 days. The tracers are started at 5.0 days.

VIII. CONCLUSION

The wave-tide forced circulation of Bay St. Louis has been examined using an iterative hydrodynamic-wave coupled model approach. It has been demonstrated that wave-current interaction is an important effect in the case of wave and tidally driven circulation since incident waves

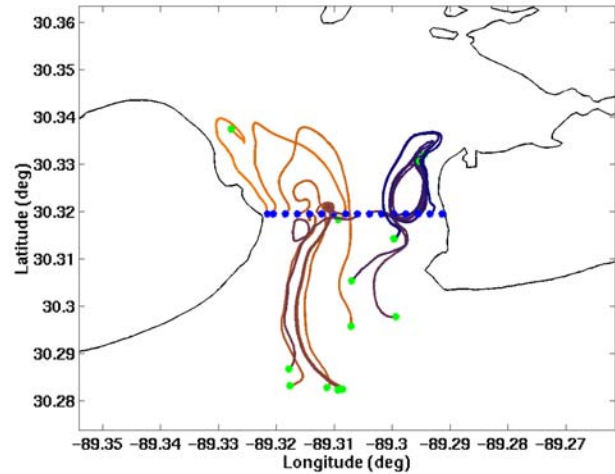


Fig. 11. The paths of passive Lagrangian tracers moving under the influence of coupled wave-tide driven currents over a time period of 0.96 days. The tracers are started at 5.0 days.

encounter strong opposing currents (which are part of the wave and tidally-induced circulation). Near the mouth of the inlet the wave-induced currents and elevation alter the tidal currents quite significantly, creating an out-flowing current during the three main phases of the tidal cycle. It has also been demonstrated that wave-induced circulation will significantly alter the transport of passive particles in tidally-driven inlets and bays. This suggests that it is important to understand the influence of wave forcing to the same extent as tidal forcing when investigating the transport of sediment, pollutants, and biological organisms in bays and inlets.

Future studies will examine the effect that changing the coupling iteration interval has on the inlet transport and circulation. In addition, radiation stress gradients obtained from true multi-spectral radiation stress will be employed for the wave forcing. Presently the wave height and direction fields are used as though they represented a monochromatic wave field. Field measurements of wave heights and directions as well as currents and elevations will also be necessary to realistically simulate the wave-tide induced circulation and calibrate the models in the regions being investigated.

Acknowledgements

The authors would like to thank Jim Kaihatu and Erick Rogers of the Naval Research Laboratory (code 7322), Stennis Space Center, MS for their help with the SWAN wave model calculations. This work is supported by the Naval Research Laboratory 6.2 Program Element 0602435N.

REFERENCES

- [1] Mark Cobb and Cheryl Ann Blain, "A Coupled Hydrodynamic-Wave Model for Simulating Wave and Tidally-Driven 2D Circulation in Inlets", Proceedings of

the 7th International Conference on Estuarine and Coastal Modeling 2001 (in press).

- [2] Luettich, R. A., J. J. Westerink, and N. W. Scheffner. (1992). "ADCIRC: An Advanced Three-Dimensional Circulation Model for Shelves, Coasts, and Estuaries, Report 1: Theory and Methodology of ADCIRC-2DDI and ADCIRC-3DL." Technical Report DRP-92-6, U.S. Army Corps of Engineers Waterways Experimental Station, Vicksburg, MS 137 pp.
- [3] Westerink, J. J., C. A. Blain, R. A. Luettich, and N. W. Scheffner. (1994a). "ADCIRC: An Advanced Three-Dimensional Circulation Model for Shelves, Coasts, and Estuaries, Report 2: User's Manual for ADCIRC-2DDI." Technical Report DRP-92, Department of the Army.
- [4] Blain, C. A., J. J. Westerink, and R. A. Luettich. (1994). "The influence of domain size on the response characteristics of a hurricane storm surge model." *J. Geophys. Res.*, 99, C9, 18467-18479.
- [5] Kolar, R. L., J. J. Westerink, M.E. Cantekin, and C. A. Blain. (1994). "Aspects of nonlinear simulations using shallow water models based on the wave continuity equation." *Computers and Fluids*, 23, 523-538.
- [6] Westerink, J. J., R. A. Luettich, and J. C. Muccino. (1994b). "Modeling tides in the western north Atlantic using unstructured graded grids." *Tellus*, 46A, 178-199.
- [7] Blain, C. A., J. J. Westerink, and R. A. Luettich. (1998). "Grid convergence studies on the prediction of hurricane storm surge." *Int. J. Num. Methods Fluids*, 26, 369-401.
- [8] Longuet-Higgins, M. S., and R. W. Stewart. (1964). "Radiation stresses in water waves; A physical discussion, with applications." *Deep Sea Research, Vol. 11*, 529-562.
- [9] Kolar, R. L. and W. G. Gray. (1990). "Shallow water modeling in small water bodies." *Proc. 8th Int. Conf. Comp. Meth. Water Res.*, Springer-Verlag, Berlin, 149-155.
- [10] Booij, N., R. C. Ris, and L. H. Holthuijsen. (1999). "A third-generation wave model for coastal regions, Part 1, Model description and validation." *J. Geophys. Res.*, 104, C4, 7649-7666.
- [11] Veeramony, Jayaram, and Cheryl Ann Blain. (2001). "Barotropic Flow in the Vicinity of an Idealized Inlet – Simulations with the ADCIRC Model." NRL/FR/7320-01-9977.